INTERNAL MEDICINE

□ ORIGINAL ARTICLE □

Echoic Features of Lymph Nodes with Sarcoidosis Determined by Endobronchial Ultrasound

Naoyuki Imai[1], Kazuyoshi Imaizumi[2], Masahiko Ando[3], Tomoya Shimokata[1], Tomomi Ogawa[1], Satoru Ito[1], Naozumi Hashimoto[1], Mitsuo Sato[1], Masashi Kondo[1] and Yoshinori Hasegawa[1]

Abstract

Objective Endobronchial ultrasound-guided transbronchial needle aspiration (EBUS-TBNA) is a minimally invasive technique with a high diagnostic yield used in the investigation of mediastinal diseases including sarcoidosis. Although previous reports have discussed the echoic features of metastatic mediastinal lymph nodes in lung cancer, few have addressed those features of mediastinal lymph nodes with sarcoidosis. We therefore investigated whether the echoic features of lymph nodes with sarcoidosis are distinct when compared to those of metastatic lymph nodes in lung cancer.

Methods This retrospective analysis was held in one university hospital between April 2007 and June 2011. EBUS-guided biopsies were performed on 219 patients, and thus resulting in sarcoidosis diagnoses in 53 patients. We quantitatively analyzed the echoic morphologic features of 42 lymph nodes from 34 sarcoidosis patients and 59 lymph nodes from 44 patients with lung cancer using digital image analyzing software.

Results In patients with sarcoidosis, 64.3% of the lymph nodes had a round shape, 71.4% had a distinct margin, and 88.1% exhibited homogeneous echogenicity. A germinal center structure was observed in 71.4% of the cases. In the context of shape and margin, no significant difference could be observed between sarcoidosis and lung cancer metastasis. However, homogeneous low echogenicity and the presence of a germinal center structure were observed in sarcoidosis more frequently than in lung cancer.

Conclusion Homogeneous low echogenicity and the presence of a germinal central structure may be distinctive echoic features of lymph nodes with sarcoidosis. Analyzing the echogenicity of the mediastinal lymph nodes may help to distinguish sarcoidosis from lung cancer.

Key words: sarcoidosis, EBUS-TBNA, ultrasound image, lung cancer metastasis

(Intern Med 52: 1473-1478, 2013)
(DOI: 10.2169/internalmedicine.52.9082)

Introduction

Sarcoidosis is a multisystem granulomatous disorder of unknown etiology and is characterized pathologically by the presence of noncaseating granulomas in the involved organs (1). Recently, endobronchial ultrasound-guided transbronchial needle aspiration (EBUS-TBNA) has been discussed as a new tool for sampling histological tissues from mediastinal lymph nodes including pulmonary sarcoidosis (2-4). The main advantage of EBUS-TBNA is being able to see the real-time echoic view of the tissues during the biopsy (5-8). However, the ultrasound (US) findings specific to lymph nodes with sarcoidosis have not yet been well documented. In this study, we compared the echoic features of mediastinal lymph nodes with sarcoidosis to those with lung cancer.

[1]Department of Respiratory Medicine, Nagoya University Graduate School of Medicine, Japan, [2]Division of Respiratory Medicine and Clinical Allergy, Department of Internal Medicine, Fujita Health University, Japan and [3]Center for Advanced Medicine and Clinical Research, Nagoya University Hospital, Japan
Received for publication October 8, 2012; Accepted for publication March 5, 2013
Correspondence to Dr. Kazuyoshi Imaizumi, jeanluc@fujita-hu.ac.jp

Materials and Methods

Patients

This was a retrospective study including 42 lymph nodes from 34 patients with sarcoidosis, and 59 lymph nodes from 44 patients with lung cancer who had mediastinal or hilar lymphadenopathy diagnosed by EBUS-TBNA at our institute between April 2007 and June 2011. The diagnosis of sarcoidosis was established when both the histological evidence of noncaseating epithelioid cell granulomas and the compatible clinicoradiological findings were demonstrated after any other known causes producing granulomatous lesions were excluded. The institutional review board of our institute approved this retrospective chart review study without our need to obtain informed consent.

Bronchoscopy

A convex probe for EBUS (CP-EBUS) bronchoscopes was used (BF-UC260-FW; Olympus; Tokyo, Japan). Ultrasound images were processed with an ultrasound scanner (EU-ME1; Olympus), and the size of the lesions could be measured by the placement of cursors. The CP-EBUS has a convex transducer (7.5 MHz) that can scan parallel to the insertion direction of the bronchoscope. The ultrasound images could be seen on the monitor and recorded as JPEG files or digital DVD files by a DVD recorder (DVO-1000M; SONY; Tokyo, Japan). The outer diameter of the CP-EBUS bronchoscope was 6.7 mm and the inner diameter of the instrument channel was 2.0 mm. A 22-gauge (22 G) needle (NA-201SX-4022, Olympus) was used for the transbronchial needle aspiration (TBNA). The needle could be visualized through the optics and the ultrasound image. We also performed bronchoalveolar lavage (BAL) in all patients. The decision to perform a trans-bronchial lung biopsy (TBLB) in some patients suspected of having sarcoidosis was left to the discretion of the operator. In addition, bronchoscopes (BF 260, Olympus) were used for both the BAL and the TBLB procedures.

Procedure

All of the bronchoscopic examinations were performed under conscious sedation with midazolam. Local anesthesia was achieved with 5 mL of nebulized 2% lidocaine solution to the pharynx. Additionally, 1% lidocaine was administered through the bronchoscopic channel during the procedure when necessary. The electrocardiogram readings, arterial oxygen saturation levels (SpO_2), exhaled CO_2 concentrations, and blood pressures were monitored in all patients. After visualization of the ultrasound image of the targeted lymph node was achieved, a 22 G needle was used to penetrate the bronchial wall through the bronchoscopic channel. The internal stylet was then removed and negative pressure was applied with a syringe. The operator moved the needle back and forth twenty times with a continuous negative pressure under the monitoring real-time US image of the lymph node. After the needle was retrieved, the internal stylet was reinserted and used to push out the histologic core. Using these methods, we obtained tissues sufficient for pathological analyses from all cases.

For patients with suspected sarcoidosis, we changed the bronchoscope (BF260) to perform the BAL on the right middle lobe bronchus or lingular lobe bronchus. Saline in 50-mL aliquots was administered and collected three times manually through the bronchoscopic channel wedged to the bronchus. When performed, the BAL followed the EBUS-TBNA procedure in all cases. As bleeding during the EBUS-TBNA was minimal and the punctures were performed at the trachea or main bronchus, we could not recognize any significant blood contamination in BALF. In addition, it was difficult to insert the CP-EBUS bronchoscope without an endotracheal intubation after the BAL was performed using a BF-260 bronchoscope.

The aspirated material was smeared onto glass slides and immediately air-dried for Giemsa staining or fixed in 95% alcohol for Papanicolaou staining. The TBNA needles were rinsed with saline for cytological and bacteriological examinations. The needle rinse fluid was smeared onto glass slides by cyto-centrifugation (Cytospin 2; Shanon Ltd., Runcorn, UK) and immediately air-dried for Giemsa staining or fixed in 95% alcohol for Papanicolaou staining. The histologic cores were fixed in 10% formalin and evaluated by hematoxylin and eosin staining.

US image analysis

Three individuals (N.I, T.S, K.I) blinded to the pathological results reviewed digital images of lymph nodes and representative still images from DVD files of US images. Per Fujiwara's criteria (9), the US images of lymph nodes were classified according to the following categories: 1) shape (oval or round), 2) margin (distinct or indistinct), 3) echogenicity (homogeneous or heterogeneous), and 4) germinal central structure (presence or absence). When the ratio of the long axis diameter to the short axis diameter of the lymph node was ≥2, we defined the node as oval. When the ratio was <2, we defined it as round. When more than 50% of the margin was clearly visualized with a high echoic border, we defined the node margin as distinct. The germinal central structure was seen in the center of the node as a linear, flat, and hyperechoic area (2). To evaluate the echogenicity quantitatively, we used an image analyzing software "ImageJ" (available at http://rsb.info.nih.gov/ij/). Using this software, we could measure the minimum, maximum, and mean pixel value of the inner space of the lymph nodes. To measure pixel values, we selected a cross-sectional view at which we biopsied the lymph node just before the needle was inserted. Avoiding the germinal center structure, at least three different fields surrounded by the user-defined square were determined for analyses (Fig. 1). Each field was determined to include more than 3,000 pixels. We measured the mean pixel value and the standard deviation per field. We

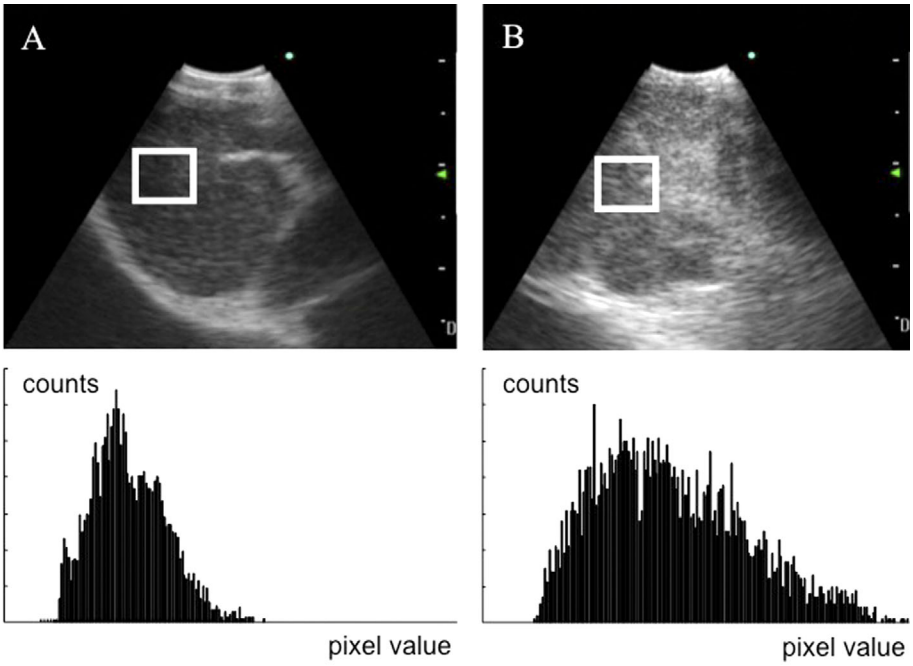

Figure 1. **Measurement of the pixel gray value in lymph nodes. Upper column: Representative US images of lymph nodes (with a square being a randomly selected, user-defined square). Lower column: Histograms of pixel values within the selected square. A: sarcoidosis; B: lung cancer. We used an image analyzing software to quantitatively evaluate the echogenicity. At least three different fields were randomly selected for analyses by the user-defined square on a cross-sectional view of the node just before needle insertion. We measured the mean pixel value of three or more fields and calculated the average.**

used the standard deviation of the pixel value at each field to evaluate the heterogeneity. The final characteristics of the US findings for each lymph node were determined based on an agreement of three reviewers (N.I, T.S, K.I).

Imaging tests

Chest and upper abdominal CT scans (Aquilion TSX-101 A, Toshiba Medical Co., Ltd., Tokyo, Japan) were performed on all patients before EBUS examination. The slice thickness was 1-mm with a pitch, and the images were reconstructed. We selected target lymph nodes where the following criteria were satisfied: 1) having a short axis >10 mm, 2) reachable from the trachea or the main bronchus, and 3) located away from major vessels. FDG-PET scans (Eminence B, Shimadzu Co., Ltd., Kyoto, Japan) were also performed on 10 patients with sarcoidosis.

Statistical analysis

Differences in the mean values between the two groups were evaluated with the Mann-Whitney *U* test. A p value of <0.05 was considered statistically significant. Mann-Whitney *U* tests and chi-square tests were used for the comparison of US findings in sarcoidosis lymph nodes with those of lung cancer. A Receiver Operating Characteristic (ROC) curve analysis was performed to decide the cutoff value of the standard deviation (SD). The best cutoff point was determined on the basis of the highest likelihood ratio and an analysis of the ROC curve. The likelihood ratio was calculated as follows: *Likelihood ratio = sensitivity/(1-specificity)*. All statistical matters were calculated using the Stat View (ver.5.0, SAS Institute; Cary, NC) software program.

Results

Between April 2007 and June 2011, we made diagnoses of sarcoidosis in 53 patients using EBUS-guided needle biopsy. We obtained digital images of 42 lymph nodes from 34 of these patients. During the same period, we also obtained digital images of 59 metastatic lymph nodes from 44 patients with lung cancer, diagnosed by EBUS-TBNA. The characteristics of the studied patients and the laboratory data are summarized in Table 1. The size and location of the lymph nodes are summarized in Table 2. There were no severe complications related to any of the bronchoscopic examinations.

We performed TBLB on 6 of 18 patients with stage I sarcoidosis and on 10 of 16 patients with stage II sarcoidosis. We demonstrated epithelioid granuloma in lung biopsy specimens from only four patients with stage II sarcoidosis. FDG-PET scans were performed on 10 patients with sarcoidosis. The median value of the SUVmax of the targeted lymph nodes was 7.7 (range, 4.6-10.1), thus showing a high uptake indistinguishable from lung cancer metastatic lymph nodes.

The characteristics of echoic findings of sarcoidosis lymph nodes are shown in Table 3. We compared these

Table 1. Characteristics of Patients Included in This Study

Patient Characteristics	sarcoidosis	lung cancer
Number of patients	34	44
Gender (male: female)	8:26	36:8
Age, y, median (range)	62 (31-75)	67 (50-86)
Radiological stage Stage I: Stage II	18 : 16	
Granuloma proven by TBLB (positive : negative : not performed)	4 : 12 : 18	
Histological type of lung cancer (Ad : Sq : NSCLC : SCLC)		17 : 13 : 6 : 8
Serum ACE, IU/mL, median (range)	26.8 (3.1-75.5)	
BALF cell counts, median (range) x10^4/mL	12.0 (1.0-37.0)	
Proportion of lymphocyte in BALF, median (range) %	26.6 (10.0-76.6)	
CD 4/8 ratio of BAL lymphocytes, median (range)	5.93 (1.3-18.6)	

Ad: adenocarcinoma, Sq: squamous cell carcinoma, NSCLC: non-small cell carcinoma, SCLC: small cell carcinoma, ACE: angiotensin-converting enzyme, BALF: bronchoalveolar lavage fluid

Table 3. Comparison of Echoic Findings of Lymph Nodes with Sarcoidosis and Lung Cancer

Findings		Sarcoidosis (n=42)	Lung cancer (n=59)	p value
Shape	Round	27	51	
	Oval	15	8	0.089
Margin	Distinct	30	33	
	Indistinct	12	26	0.113
Echogenicity	Homogeneous	37	19	
	Heterogeneous	5	40	< 0.001
Germinal center structure	Present	30	16	
	Absent	12	43	< 0.001

characteristics with those of metastatic lymph nodes of lung cancer diagnosed by the EBUS-TBNA method in our institute during the same time period (Table 3). In terms of lymph node shape and margin, there were no statistical differences between these two diseases. However, the majority of the sarcoidosis lymph nodes (88.1%) showed homogeneity, while a large proportion of the lymph nodes with lung cancer (67.8%) showed heterogeneous echogenicity. Germinal central structures could be seen in many cases of sarcoidosis (71.4%), but not in lung cancer (27.1%). We found significant differences in the echogenicity and in the presence of germinal center structure between sarcoidosis and lung cancer ($p<0.01$) (Table 3).

To confirm the difference in echogenicity of lymph nodes between sarcoidosis and lung cancer, we measured the pixel values of the lymph nodes studied using the digital analyzing software "ImageJ". Briefly, we evaluated the mean and the distribution of pixel values in the square field randomly selected at each targeted lymph node (Fig. 1). The SD of the pixel value at each square was calculated for the analysis of the echogenic heterogeneity of the lymph nodes (Figs. 1, 2, Table 4). The mean pixel value of sarcoidosis (61.1) was significantly lower than that of lung cancer (77.8) ($p<0.001$). The SD of echogenicity in sarcoidosis lymph nodes was 12.4, and that of lung cancer was 21.4 (Fig. 2, Table 4). The difference was also significant, thus indicating that sarcoidosis lymph nodes have lower and more homogeneous echoic features than lung cancer lymph nodes.

Table 2. Lymph Node Stations of Patients with Sarcoidosis and Lung Cancer Included in This Study

Lymph node station	sarcoidosis	lung cancer
All	42	59
2R	0	2
4L	4	5
4R	18	25
7	17	14
10R	1	6
11R	2	3
other	0	4
Long axis of node, mean (range)	25.3 (13-61) mm	20.7 (10-43) mm
Short axis of node, mean (range)	16.4 (11-26) mm	29.1 (12-57) mm

Table 4. Comparative Evaluation of Pixel Values of Each Lymph Node in Sarcoidosis and Lung Cancer

	Sarcoidosis	Lung cancer	p
Minimal value, mean (range)	28.3 (18-49)	32.7 (20-67)	0.53
Maximum value, mean (range)	122.2 (81-182)	144.4 (93-212)	0.03
Mean value, mean (range)	61.1 (16.7-85.3)	77.8 (39.8-118.3)	< 0.01
Standard deviation, mean (range)	12.4 (8.1-20.2)	21.4 (11.9-33)	< 0.01

We determined the best cut-off value of SD as a marker to distinguish sarcoidosis from lung cancer using receiver operating curve (ROC) curve analysis (Fig. 3). When the cut-off value of SD was 15, the sensitivity was 88.1%, the specificity was 93.2%, the accuracy was 91.1%, the positive predictive value was 90.2%, the negative predictive value was 91.7%, the positive relative rate was 10.83, the negative relative rate was 9.39, the area under the ROC was 0.965, and the diagnostic odds ratio was 101.5. We also evaluated echogenicity (mean pixel value) as a marker to distinguish these two diseases (lung cancer and sarcoidosis), but all results were more accurate when we used SD. According to these results, we speculate that homogeneous low echogenicity and the presence of germinal central structure might thus be distinctive echoic features of lymph nodes with sarcoidosis.

Discussion

Recently, many investigators have reported that EBUS-TBNA is one of the most appropriate methods for diagnosing mediastinal lymphadenopathies including sarcoidosis (8-12). Because of the lower invasiveness and high diagnostic ability, EBUS-TBNA will likely become the essential procedure for the diagnosis of mediastinal diseases (13, 14). However, in many cases with lung cancer or sarcoidosis, there are multiple enlarged lymph nodes. In addition, some lung cancer cases may have non-metastatic lymphadenopathy that must be differentiated from lymph node metastases (15). As it is difficult to obtain pathological samples from all lymph nodes, sonographic features may be very useful for evaluating mediastinal lymph nodes.

Fujiwara et al. reported how to evaluate echoic findings obtained via EBUS in lung cancer (9). They reported that mediastinal metastatic lymph nodes have four characteristic

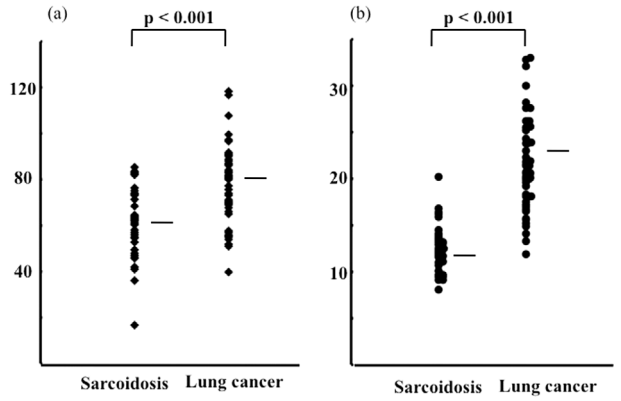

Figure 2. **Comparison of lymph node digital images between sarcoidosis and lung cancer. (a) Distribution of the mean pixel value in each lymph node. (b) Distribution of the mean standard deviation of the pixel value in each lymph node.**

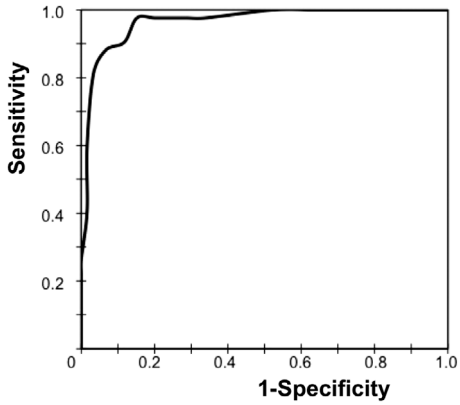

Figure 3. **ROC curve analysis of the accuracy of the standard deviation as a marker to distinguish sarcoidosis and lung cancer. The best cutoff point was determined on the basis of the highest likelihood ratio and an analysis of ROC curve.**

sonographic features including round shape, distinct margin, heterogeneous echogenicity, and the presence of a coagulation necrotic sign.

In the present study, we evaluated the echoic features of lymph nodes in sarcoidosis patients including the objective analysis of echogenicity using 'ImageJ.' As we chose only lymph nodes with a short axis of more than 10-mm in length as EBUS-TBNA targets, we did not evaluate the size of each lymph node in this study. Our study demonstrated that mediastinal lymph nodes of sarcoidosis tend to have sonographic characteristics including: 1) round shape, 2) distinct margin, 3) homogeneous echogenicity, and 4) a germinal center structure. In addition, the digital image analyses showed that sarcoidosis lymph nodes have a lower and more homogeneous echogenicity compared to those of lung cancer. Intriguingly, we could not find significant differences in the shape and the margin of the lymph nodes with sarcoidosis or lung cancer. We speculated that 'round shape' and 'distinct margin' are characteristic features of lymphadenopathy accompanied not only by malignancy but also benign diseases. However, there was a statistical difference in the echogenicity and the echoic features of the inner part of the lymph nodes, (e.g., the presence of a central hilar structure) with either sarcoidosis or lung cancer. The ImageJ software program was used to calculate the pixel values and to make histograms of defined regions in the sonographic examination. According to previous reports, it is useful to use ImageJ software to analyze the ultrasonographic images (16-18). In this study, we used the standard deviation of the echogenicity of each defined region for sonographic heterogeneity because it was clear and easy to estimate (16). Nguyen et al. discussed the efficacy of analyzing echoic features via EBUS-TBNA using ImageJ and MATLAB (ver.7.9.0.529, The Mathworks) (18). They concluded that analyses of echo findings were helpful for distinguishing the malignant lymphadenopathies from the benign lymphadenopathies. They reported the same parameters useful when distinguishing between malignant and benign diseases, including the standard error of mean (SEM), correlation, energy, entropy, and the difference between maximal and minimal pixel values. In our study, we used SD to estimate the echogenicity of lymph nodes. Although our focus was on sarcoidosis, a single disease, in comparison with lung cancer, the method using SD is simpler and has higher diagnostic yields than the previous report.

During the reviewed period, the performance of a TBLB procedure in addition to the EBUS-TBNA was left to the discretion of the operator. A recent report demonstrated that the diagnostic yield of EBUS-TBNA for stage I and II sarcoidosis is higher than that of TBLB (11), and should therefore be the first line of investigation of sarcoidosis. We confirmed that report when we could identify epithelioid granuloma in lung biopsy specimens from only 40% of studied patients with stage II sarcoidosis.

Our study has some limitations. First, ours is a retrospective review with a limited number of patients. Although our investigation shows the echoic characteristics of sarcoidosis lymph nodes, additional studies with more patients are warranted. Second, we could not compare the echoic findings of sarcoidosis with other malignant or benign diseases such as tuberculosis or malignant lymphoma. During the study period, we found a very limited number of cases with these diseases (only two cases of lymphoma, and only one of these cases had an evaluable digital record). More US images of lymphadenopathy from various diseases are therefore needed for a comprehensive review. Third, the evaluation of the echoic features by "ImageJ" in our study does not involve real-time performance. The bronchoscopes and ultrasound image scanning and processing systems now in use do not have any equipment or software to evaluate the echoic density of the images in real time. The development of such equipment should therefore be our goal.

In conclusion, low and homogeneous echogenicity is a distinct sonographic feature of lymph nodes with sarcoidosis rather than lung cancer metastasis. Although further studies of US findings in lymph nodes from other diseases are

needed, the analysis of the echoic findings of lymph nodes via EBUS-TBNA may be useful for the differential diagnosis of mediastinal lymphadenopathy.

The authors state that they have no Conflict of Interest (COI).

Acknowledgement

This study was supported in part by a Grant-in-Aid for Scientific Research from the Japan Society for the Promotion of Science.

References

1. ATS/ERS/WASOG Committee. ATS/ERS/WASOG statement on sarcoidosis. Am J Respir Crit Care Med **160**: 736-755, 1999.
2. Yasufuku K, Chiyo M, Sekine Y, et al. Real-time endobronchial ultrasound-guided transbronchial needle aspiration of mediastinal and hilar lymph nodes. Chest **126**: 122-128, 2004.
3. Herth FJ, Eberhardt R, Vilmann P, Krasnik M, Ernst A. Real-time endobronchial ultrasound guided transbronchial needle aspiration for sampling mediastinal lymph nodes. Thorax **61**: 795-798, 2006.
4. Herth F, Becker HD, Ernst A. Conventional vs endobronchial ultrasound-guided transbronchial needle aspiration: a randomized trial. Chest **125**: 322-325, 2004.
5. Wong M, Yasufuku K, Nakajima T, et al. Endobronchial ultrasound: new insight for the diagnosis of sarcoidosis. Eur Respir J **29**: 1182-1186, 2007.
6. Garwood S, Judson MA, Silvestri G, Hoda R, Fraig M, Doelken P. Endobronchial ultrasound for the diagnosis of pulmonary sarcoidosis. Chest **132**: 1298-1304, 2007.
7. Oki M, Saka H, Kitagawa C, et al. Real-time endobronchial ultrasound-guided transbronchial needle aspiration is useful for diagnosing sarcoidosis. Respirology **12**: 863-868, 2007.
8. Nakajima T, Yasufuku K, Kurosu K, et al. The role of EBUS-TBNA for the diagnosis of sarcoidosis--comparisons with other bronchoscopic diagnostic modalities. Respir Med **103**: 1796-1800, 2009.
9. Fujiwara T, Yasufuku K, Nakajima T, et al. The utility of sonographic features during endobronchial ultrasound-guided transbronchial needle aspiration for lymph node staging in patients with lung cancer: a standard endobronchial ultrasound image classification system. Chest **138**: 641-647, 2010.
10. Agarwal R, Srinivasan A, Aggarwal AN, Gupta D. Efficacy and safety of convex probe EBUS-TBNA in sarcoidosis: a systematic review and meta-analysis. Respir Med **106**: 883-892, 2012.
11. Oki M, Saka H, Kitagawa C, et al. Prospective study of endobronchial ultrasound-guided transbronchial needle aspiration of lymph nodes versus transbronchial lung biopsy of lung tissue for diagnosis of sarcoidosis. J Thorac Cardiovasc Surg **143**: 1324-1329, 2012.
12. Eckardt J, Olsen KE, Jørgensen OD, Licht RB. Minimally invasive diagnosis of sarcoidosis by EBUS when conventional diagnostics fail. Sarcoidosis Vasc Diffuse Lung Dis **27**: 43-48, 2010.
13. Poletti V, Tomassetti S. Ultrasound endoscopy (EBUS, EUS) as a sophisticated tool for morphological confirmation of sarcoidosis: do we need to find new answers for an old quest? Sarcoidosis Vasc Diffuse Lung Dis **27**: 5-6, 2010.
14. Gilbert S, Wilson DO, Christie NA, et al. Endobronchial ultrasound as a diagnostic tool in patients with mediastinal lymphadenopathy. Ann Thorac Surg **88**: 896-900, 2009.
15. Steinfort DP, Irving LB. Sarcoidal reactions in regional lymph nodes of patients with non-small cell lung cancer: incidence and implications for minimally invasive staging with endobronchial ultrasound. Lung Cancer **66**: 305-308, 2009.
16. Chou SY, Chen CY, Chow PK, Hsu CS, Hsu MI, Chiang HK. Ultrasonographic evaluation of endometrial changes using computer assisted image analysis. J Obstet Gynaecol Res **36**: 634-638, 2010.
17. Irving BA, Weltman JY, Brock DW, Davis CK, Gaesser GA, Weltman A. NIH ImageJ and Slice-O-Matic computed tomography imaging software to quantify soft tissue. Obesity **15**: 370-376, 2007.
18. Nguyen P, Bashirzadeh F, Hundloe J, et al. Optical differentiation between malignant and benign lymphadenopathy by grey scale texture analysis of endobronchial ultrasound convex probe images. Chest **141**: 709-715, 2012.